Published in : Engineering Structures (2024), vol. 315, 118460
DOI: 10.1016/j.engstruct.2024.118460
Status : Postprint (Author's version)

Improvement of the prediction of the flexural buckling resistance of hot-rolled mild and high-strength steel members

Loris Saufnay*, Jean-Pierre Jaspart, Jean-François Demonceau

UEE Department, University of Liège, All. de la Découverte B52, 4000 Liège, Belgium

Keywords:

High-strength steels
Flexural buckling
Buckling curves
Hot-rolled sections
Finite element simulations
Design rules

Abstract

The determination of the bearing capacity of a member under compression, presenting an initial out-of-straightness and residual stresses resulting from the production process, is a stability problem governed by the geometry of the member and the mechanical properties of its constitutive material. Amongst these, the yield strength plays a key role. Indeed, it has a direct impact on the spread of yielding in the member but, also, the detrimental effect of geometrical and material imperfections decreases as the yield strength increases. The effect of these initial imperfections is considered by an imperfection factor α in the design recommendations provided in EN1993–1-1. However, the current and new upcoming versions of this norm give a stepwise evolution of this imperfection as a function of yield strength by only distinguishing grades lower than S460 from the ones equal/ higher than S460. The present paper aims to briefly summarize the existing studies on this topic, to assess the recommendations of current and new upcoming versions of EN1993–1-1 and the models reported in the literature and, finally, to suggest a modified imperfection factor for hot-rolled sections (H-shape and I-shape) for already existing grades (up to S500) but also for grades up to S690, which do not exist yet for this section typology in the European steel market, to evaluate the structural benefit of developing them.

Introduction

Optimizing structures by reducing the amount of used raw materials will become more significant in the upcoming years as societies strive to optimize their use of natural resources and make it more sustainable. The steel industry is in constant evolution by promoting and developing new production technologies and materials [1]. Amongst the new materials, high-strength steels represent the highest strength-to-weight ratio of existing steels, thus providing the

Published in : Engineering Structures (2024), vol. 315, 118460
DOI: 10.1016/j.engstruct.2024.118460
Status : Postprint (Author's version)

same strength with less material weight which leads to material, cost and carbon footprint savings depending on their corresponding relative price and carbon footprint [2, 3]. Therefore, high-strength steels appear as an adequate reply to the current considerations, i.e., building with less material in a more efficient way.

In the past years, a series of RFCS European projects have already been conducted on high-strength steels [4,5,6,7,8,9,10,11] in which the structural behavior of high-strength steel members is discussed and some design rules for high-strength steels have been derived. However, most research focuses on welded I-beams and cold-formed hollow sections as yield strengths are already available at least up to 690 MPa for such sections. Indeed, for hot-rolled steel sections, only steel grades up to S500 can be found on the European steel market and 80 ksi (550 MPa) in the US steel market.

One of the well-known drawbacks of high-strength steels is the flexural buckling which limits the benefits of using them [3,12,13,14]. The flexural buckling resistance depends on two main parameters: the geometrical imperfection and the residual stresses which are accounted for through an imperfection factor defining the well-known European buckling curves. Although the geometrical imperfection is not affected by the yield strength, the detrimental effect of the residual stress distributions is reduced when the yield strength is increased. This beneficial effect of the yield strength on the bucking capacity is already accounted for in Eurocode recommendations by providing various buckling curves, i.e., different imperfection factors, but in a stepwise manner, respectively for grades lower than S460 and grades equal/higher than S460 [15]. An extension of these rules for grades from S460 up to S700 is recommended in Part 1–12 of Eurocode 3 [16] and the new upcoming version FprEN1993–1-1:2022 [17] is currently doing the same grade distinction. The lack of continuity of the imperfection factor as a function of yield strength is detrimental for steel grades between S235 and S460 and higher than S460; indeed, the imperfection factors as proposed in the codes have been calibrated for members with S235 and S460 steel grades which means that, for the other steel grades, the predictions obtained considering these coefficients are on the safe side. Having appropriate design criteria is seen as a necessity to optimize steel structures in the future and to realize material savings.

To achieve this objective, two main solutions can be contemplated: either proposing a set of buckling curves for each grade characterized by their own imperfection parameter or keeping the five existing buckling curves recommended in the Eurocodes and making them applicable for all steel grades through a modified imperfection factor defined as a function of the yield strength.

Therefore, the present paper aims to study the positive impact of the yield strength on the flexural buckling resistance of hot-rolled H-shape profiles and to propose a new formula for the imperfection factor reflecting a continuous evolution of this factor according to the yield strength. This paper also covers grades higher than S500 in a prospective study to determine the potential benefit of developing such yield strengths for hot-rolled sections.

Published in : Engineering Structures (2024), vol. 315, 118460
DOI: 10.1016/j.engstruct.2024.118460
Status : Postprint (Author's version)

Literature review

BACKGROUND OF THE EUROPEAN BUCKLING CURVES

Given that the presented investigations relate to European design recommendations for flexural buckling, the focus of the literature review is made on previous European works. According to the design recommendations of Eurocode 3 [15], the resistance of an element subjected to compression is checked using Eq. 1:

$$N_{b,Rd} = \frac{\chi * \beta * A * f_y}{\gamma_{M1}} \geq N_{Ed} \quad (1)$$

where $N_{b,Rd}$ is the design buckling resistance, N_{Ed} the design value of the compression force, χ the reduction factor to account for the risk of flexural buckling, β the reduction factor to account for the risk of local plate buckling, A the cross-sectional area, f_y the yield strength and γ_{M1} the partial safety coefficient for stability problems.

Both geometrical imperfections and residual stresses negatively affect the behavior of compressed columns. A correct description of the column buckling phenomenon therefore requires considering these geometrical and material imperfections. The European buckling curves $\chi = f(\bar{\lambda})$ were introduced for this purpose as a practical design tool. These curves provide characteristic resistance values based on more than 1000 experimental tests performed under the auspices of the European Convention for Constructional Steelwork (ECCS) in various European countries in the '60 s [18] and on a theoretical study on which the curves are based [19]. These experimental and numerical campaigns led to a proposition of buckling curves for which the safety has been assessed by Monte-Carlo simulations [20]. Finally, Maquoi and Rondal derived the current Ayrton-Perry format of the buckling curves [21], which is still used nowadays for designs. This formulation is expressed here below.

$$\chi = \frac{1}{\phi - \sqrt{\phi^2 - \bar{\lambda}^2}} \quad \text{with } \phi = 0.5 * (1 + \eta + \bar{\lambda}^2) \quad \text{and } \eta = \alpha * (\bar{\lambda} - 0.2) \quad (2)$$

with η the imperfection parameter, α the imperfection factor and $\bar{\lambda}$ the relative slenderness.
A half-sinusoidal out-of-straightness of L/1000 as well as residual stresses according to the section typology are accounted for through an imperfection parameter α. This amplification value of L/1000 was already proposed in 1894 [22] and was confirmed by several measurements during the wide experimental campaign in the '60 s. This parameter α can take different values according to EN1993–1-1 [15] as listed in Table 1.

The buckling curve selection depends on the cross-section shape, the buckling axis, the cross-section height-to-width h/b ratio, the flange thickness t_f and the production process that influences the residual stress pattern, and therefore the buckling resistance of the member.

Published in : Engineering Structures (2024), vol. 315, 118460
DOI: 10.1016/j.engstruct.2024.118460
Status : Postprint (Author's version)

MODIFIED IMPERFECTION FACTORS FROM THE LITERATURE

The buckling curves were originally established based on a fictitious material characterized by an elastic limit $f_y = 255$ MPa. Indeed, the experimental campaign was realized in the '60 s using mild steels with low thickness (below 40 mm) while only a few tests were performed on higher steel grades, equivalent to current S275 and S355. It was concluded at that time that the yield strength had little influence on the dimensionless buckling curves, which justifies that they were established for a fixed value of 255 MPa [19].

In opposition to this statement, it was later shown that residual stress distributions do not evolve proportionally with the yield strength, leading to an increase in buckling resistances for higher grades as the local yielding is delayed. For hot-rolled cross-sections, the residual stresses depend effectively on the geometrical cross-section properties and the cooling rate during the production process and are definitively not proportional to the yield strength [23] as confirmed by experimental investigations [24]. In fact, the residual stress-to-yield strength ratio decreases when the yield strength increases. It could therefore have been decided to define the imperfection factor as a function of the yield strength to consider the beneficial effect of an increasing yield strength on the member buckling resistance. In 1976, the ECCS recommendations [25] allowed a jump of one buckling curve when the yield stress reaches 430 MPa. Maquoi established a yield strength-dependent expression of the imperfection factor [26] based on these recommendations, respecting the "jump" between mild and high-strength grades.

$$\alpha^* = \alpha * \left(\frac{235}{f_y}\right)^{0.8} \qquad (3)$$

The value of 255 MPa could have been adopted instead of 235 MPa for the sake of consistency with the value on which the buckling curves are based [27]. However, in 1982 [26], Maquoi decided to consider S235 as the reference, together with an exponent of 0.8 to respect the jump of one buckling curve preconized in the ECCS recommendations. In this manner, if $\alpha = 0.34$ for S235 which corresponds to curve "b", $\alpha^* = 0.21$ for S430 which corresponds to buckling curve "a". Similarly, if $\alpha = 0.21$ for S235, $\alpha^* = 0.13$ for S430 which corresponds to buckling curve "a_0". However, when $\alpha = 0.49$ for S235 which corresponds to curve "c", $\alpha^* = 0.30$ for S430 which does not correspond to buckling curve "b". This feature was not discussed at that time and considering that this proposal was based on a limited number of experimental tests, it was therefore not implemented in design standards. The research campaign for S460 subsequently led to a beneficial adaptation of the buckling curve selection for this specific grade. So nowadays, only S460 benefits from the reduced influence of the residual stresses for higher yield strength. Indeed, the curves initially established for a yield stress of 255 MPa were considered applicable without modifications for grades up to S420 while grade S460 got preferential treatment; this is still the case in both Eurocode versions [15,17]. In some cases, the buckling curve a_0 is even recommended for S460 whereas this curve was originally established for sections without any residual stresses [19] the subscript 0 means "zero residual stresses" - which demonstrates the inconsistency of the currently proposed discrete buckling curves [27]. Intermediary grades between S235 and S460 may deserve higher buckling curves than the ones currently preconized, what will be demonstrated in the present paper.

TABLE 1

Buckling curve specification according to EN1993–1-1 [15].

Published in : Engineering Structures (2024), vol. 315, 118460
DOI: 10.1016/j.engstruct.2024.118460
Status : Postprint (Author's version)

Buckling curve letter	a_0	a	b	c	d
Imperfection factor	0.13	0.21	0.34	0.49	0.76

Indeed, for several years, given the number of experimental and numerical investigations about the structural behavior of members made of high-strength steels [28,29,30,31,32,33,34,35,36], some authors [26,29,37,38,39] have proposed new expressions of the imperfection parameter η (see Eq. 2) in which the influence of the yield strength is explicitly accounted for. The proposed equations for the imperfection parameter are listed by section typologies in Table 2.

According to Table 2, there exist different approaches for considering the influence of the yield strength in the imperfection factor:

- The first approach consists in proposing a modified imperfection factor, noted α^* in the following form: $\alpha^* = \alpha * \left(\frac{235}{f_y}\right)^n$; this approach has been the most promoted one in the literature for decades. Indeed, Maquoi already proposed this format in 1982 [26] and it was later recommended in an IABSE report in a generalized form [40]. In 2005, the exponent n = 1 was seen as more suitable for grades up to S400 while Maquoi was recommending an exponent n = 0.8 [26]. The main advantages of this form for the modified imperfection factor are; (i) to keep the same historical buckling curves for S235 and (ii) to avoid proposing different specific imperfection factor values for each steel grade. The exponent could be different depending on the section typology as illustrated in Table 2.
- The second approach consists of applying a coefficient $\varepsilon = \sqrt{\frac{235}{f_y}}$ on the relative slenderness as proposed by Jonsson and Stan ¨ [37] in 2016 for hot-rolled sections subjected to strong-axis flexural buckling. This approach consists of considering this parameter ε, which is well-known in the steel construction sector for accounting the yield strength. But, in this form, it implies that the higher the yield strength, the longer the yielding plateau. The validity of this approach for weak axis flexural buckling has not been investigated.
- The third approach consists of forgetting all current buckling curves and proposing a modified imperfection factor as a function of ε. In the publication for hollow sections from Meng and Gardner [29], they also proposed to reduce the length of the yielding plateau to a relative slenderness of 0.1, instead of 0.2.

The various approaches do not respect the current recommendations of Eurocode 3, as the first one was established to fit with 430 MPa instead of 460 MPa, the second modifies the length of the yielding plateau and the third one does not respect the historical buckling curve discretization. So, this paper presents investigations performed on the buckling resistance of members made of hot-rolled sections with the objective of proposing a consolidated model to account for the beneficial impact of high-yield strength.

Research objectives and adopted methodology

This paper aims to evaluate the effect of the yield strength on the buckling resistance of columns under compression as well as to propose a new imperfection factor expression to continuously account for the yield strength. The

Published in : Engineering Structures (2024), vol. 315, 118460
DOI: 10.1016/j.engstruct.2024.118460
Status : Postprint (Author's version)

pursued methodology consists of calculating buckling resistances based on geometrically and materially non-linear analyses with imperfections (GMNIA). These analyses are performed by using the FineLg finite element software developed by the Greisch office and the University of Liège [41]. This software has been used and validated through many studies conducted in the past to model instability phenomena [42,43,44,45,46]. The numerical investigations focus on hot-rolled sections in existing grades ranging between S235 and S500, but also in possible future emerging higher grades (up to S690), therefore in the framework of a prospective study. In addition, the scope of this study is limited to H-shape cross-sections which possess low-thickness flanges as these profiles are the most represented ones in product catalogues ($t_f \leq 40$ mm and $t_f \leq 100$ mm for height-to-width ratios above and below 1.2 respectively). The yield strength f_y of steel grades is considered equal to the recommended values in FprEN1993–1-1 [17] for grades up to S700 depending on the thickness domain, i.e., $t_f \leq 40$ mm or 40 mm < $t_f \leq 80$ mm [17]. The HISTAR® trademark steels of ArcelorMittal offer improved yield strengths up to higher flange thickness, for instance, the nominal yield strength is conserved up to 100 mm for HISTAR® 460 [47]. However, according to product standards EN10025–2 [48] and EN10025–4 [49], even for flange thicknesses below 40 mm, a small decrease in the yield strength is contemplated; the effect of this eventual reduction is also addressed in this paper by considering the yield strength associated with the maximum flange thickness as prescribed in the above-mentioned product standards (see Fig. 1).

Higher thicknesses have been already investigated in a previous study in which the negative effect of the associated yield strength reduction was observed [50]. However, only a few sections exist with thicknesses higher than 100 mm for h/b> 1.2 (already studied in [50]) while no one exists for h/b≤ 1.2 in product catalogues [50,51].

Flexural buckling about both buckling axes is studied and, to simulate a buckling curve, 13 simply supported columns are modelled corresponding to 13 various reduced slendernesses along the buckling curve; each specimen length is obtained using the Eurocode relative slenderness depending on the classification (Eq. 4):

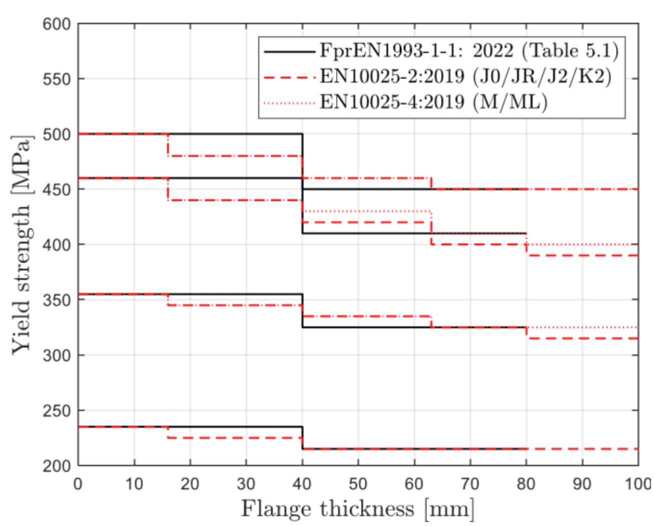

Fig. 1. Evolution of the yield strength depending on the flange thickness.

$$\overline{\lambda} = \sqrt{\frac{\beta * A_{FEM} * f_y}{N_{cr}}} \rightarrow L = L_{fl} = \frac{i * \pi * \overline{\lambda}}{\sqrt{\frac{\beta * f_y}{E}}} \quad (4)$$

Published in : Engineering Structures (2024), vol. 315, 118460
DOI: 10.1016/j.engstruct.2024.118460
Status : Postprint (Author's version)

Based on failure loads obtained by numerical simulations, the corresponding reduction factor can be derived as:

$$\chi = \frac{N_{u,FEM}}{\beta * A_{FEM} * f_y} \quad (5)$$

Where $N_{u,FEM}$ is the ultimate load obtained by numerical simulations and A_{FEM} is the area of the cross-section used in finite element simulations. The correspondence between Eurocode and numerical buckling curves is evaluated by calculating the mean value ($\bar{x}$), the standard deviation (COV) and the minimum and maximum values of the ratios ( ) between numerical and analytical reduction factors $\chi_{\chi_{FEM_{EC3}}}$. A buckling curve is assumed to be suitable when the mean value is above 1.0, this limit corresponds to the partial safety coefficient for stability design calculations (γ_{M1} = 1.0). The statistical evaluation and the figures presenting the results of the study have been realized by means of the MATLAB software [52]. Although the numerical simulations are mainly performed by using beam finite elements, when no local instabilities are expected, some shell finite element simulations are also performed to generalize the conclusions for Class 4 cross-sections. A summary of the wide numerical campaign consisting of more than 1500 columns, including geometrical properties of the selected cross-sections and the type of finite elements used depending on the EC3 cross-section classification is reported in Table 3. It is worth noting that more profiles are considered for height-to-width ratios below 1.2 to cover the wider spectrum of thicknesses (up to 100 mm). Additional numerical simulations for HEM500 and HD400×818 profiles were realized considering the yield stress reduction according to product standards EN10025–2 and EN10025–4 [48,49].

Table 3
Geometrical properties and type of finite elements for each selected cross-section.

Limits	Designation	h [mm]	b [mm]	t_w [mm]	t_f [mm]	r [mm]	Class in S460	Class in S690	Type of FE
$h/b > 1.2$ / $t_f \leq 40$ mm	HEB400	400	300	13.5	24	27	2	3	Beam
	HEM500	524	306	21	40	27	1	2	Beam
	HEB600	600	300	15.5	30	27	4	4	Shell
$h/b \leq 1.2$ / $t_f \leq 100$ mm	HEA240	230	240	7.5	12	21	3	3	Beam
	HD400×262	387	398	21.1	33.3	15	1	1	Beam
	HD400×634	474	424	47.6	77.1	15	1	1	Beam
	HD400×818	514	437	60.5	97.0	15	1	1	Beam
	HEA300	290	300	8.5	14	27	3	4	Shell

Numerical simulations using beam finite elements

DESCRIPTION OF THE NUMERICAL MODEL

Buckling curves are simulated using geometrically and materially non-linear analyses with imperfections (GMNIA). The numerical simulations are realized by imposed load at the top of the modelled column. The non-linear analysis is solved using the arc-length method in order to catch the decreasing load branch after reaching the peak load. The $N_{u,FEM}$ is considered as equal to the peak load, which corresponds to the maximum load on the load-displacement curve. 10 beam elements have been chosen to model a column based on a mesh sensitivity study. Before the non-

Published in : Engineering Structures (2024), vol. 315, 118460
DOI: 10.1016/j.engstruct.2024.118460
Status : Postprint (Author's version)

linear analysis, a linear bifurcation analysis (LBA) is performed to get the first instability mode shape. This mode shape is introduced as a geometrical imperfection and amplified by L/1000 as buckling curves were derived based on this value and as commonly recommended in many studies [20,50,51,53,54]. Regarding the residual stress patterns, the preconized distributions for hot-rolled sections from

ECCS [50,51,53] are implemented in the model, with peak stresses of

0.3 * 235 = 70.5 MPa for sections with h/b> 1.2 and

0.5 * 235 = 117.5 MPa for sections with h/b≤ 1.2. These residual stress distributions are supposed to be constant over the thickness, and the $f_y{}^*$ indicated in Fig. 2 is 235 MPa. This ECCS residual stress model is commonly used for wide flange hot-rolled sections regardless the yield strength as it has been confirmed that the yield strength is not influencing the residual stress distribution within a hot-rolled cross-section [25,37,55,56,57]. Thus, this model has been considered for each numerical model as recommended in new standard prEN1993–1-14 [58]. The assumed material model is linear elastic – perfectly plastic material model without strain hardening. A nominal plateau slope of E/10000 has been applied for numerical stability reasons. The impact of strain hardening for relative slenderness higher than 0.2 is neglectable as failure mode is a flexural buckling instability mode; this was already assumed in another research [50,54]. The assumptions behind the numerical models are summarized in Fig. 2.

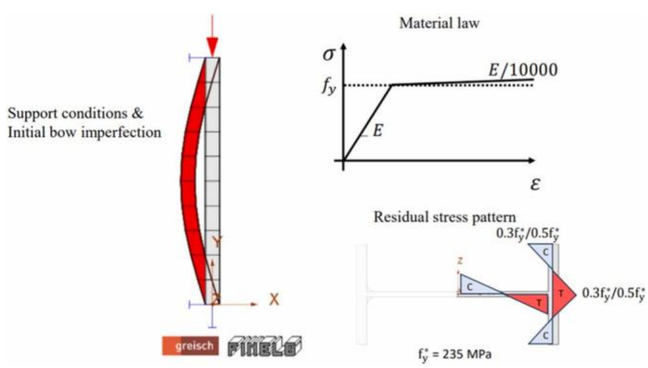

Fig. 2. Description of model assumptions for beam finite element modelling.

VALIDATION

To validate the accuracy of the developed numerical model, a comparison between numerical and experimental data has been carried out. The validation was performed on the experimental tests carried out at the Fritz Engineering Laboratory in 1972 [59]. This campaign was an extension of the ECCS program [18] targeting heavy shape cross-sections (thickness greater than 30 mm) which are covered in this study. The test program consists of buckling tests of pinned end HEM340

(*h/b* > 1.2) and W12×161 (*h/b* ≤ 1.2) columns for two different slenderness ratios (L/i_z = 50 and L/i_z = 95) and provides additional measurements (coupon tests, residual stress distribution, out-of-straightness). It has been decided to simulate numerically one test of both slenderness for the two sections to ensure the accuracy of the numerical model to simulate buckling curves; the results are represented in Fig. 3. The linear elastic material law has been used to reproduce these experimental tests to show its relevance for such simulations.

Published in : Engineering Structures (2024), vol. 315, 118460
DOI: 10.1016/j.engstruct.2024.118460
Status : Postprint (Author's version)

As shown in Fig. 3, the numerical model provides satisfactory predictions. It should be noticed that, for tests B-1-B-2–1 and B-1-GB-1–1, the numerical response is highly dependent on the residual stress pattern as the relative slenderness for these columns is close to 1.0. It is important to mention that residual stress measurements are not provided for tests B-1-B-2–1 and B-1-GB-1–1, thus the same residual stress patterns as for tests B-1-B-2–4 and B-1-GB-1–5 have been introduced leading to the observed difference in terms of peak loads. In addition, as reported in Fig. 3, other numerical simulations have been performed by considering predefined imperfections, i.e., the ECCS residual stress model and a geometrical imperfection of L/1000 to illustrate the correspondence between numerical simulations and Eurocode predictions.

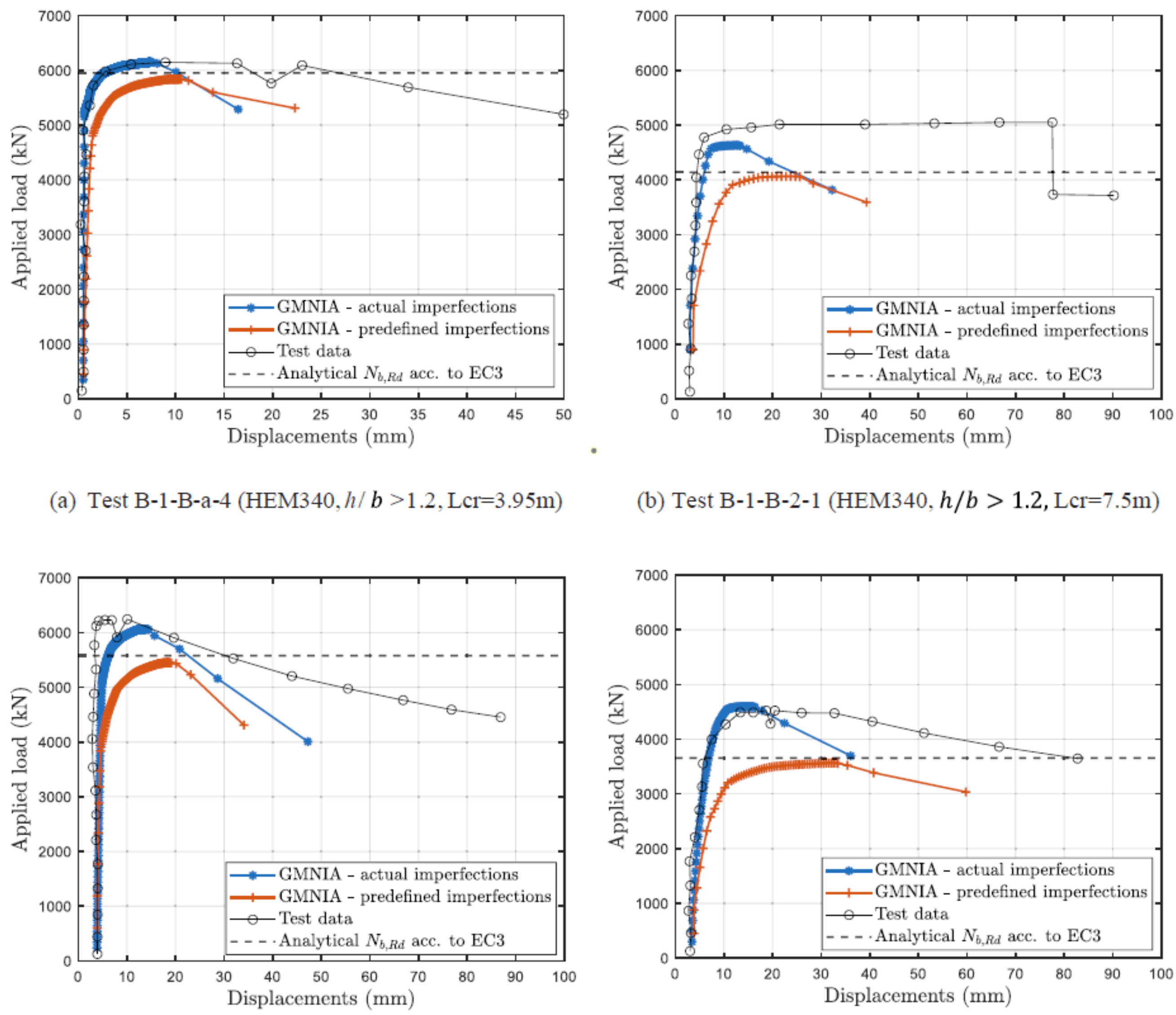

(a) Test B-1-B-a-4 (HEM340, h/b >1.2, Lcr=3.95m)

(b) Test B-1-B-2-1 (HEM340, $h/b > 1.2$, Lcr=7.5m)

(c)Test B-1-GB-1-5 (W12x161, $h/b \leq 1.2$, Lcr=4.06m)

(d) Test B-1-GB-1-1 (W12x161, $h/b \leq 1.2$, Lcr=7.7m)

Fig. 3. Validation of the numerical model based on experimental results.

Published in : Engineering Structures (2024), vol. 315, 118460
DOI: 10.1016/j.engstruct.2024.118460
Status : Postprint (Author's version)

This validation was conducted on the existing buckling tests for mild steels, as no buckling test results on hot-rolled double-T members in high-strength steels are available in the literature. However, another study has already demonstrated the reliability of this finite element software to simulate the flexural buckling of hot-rolled high-strength angles members [45]. As the aforementioned research focuses on a different cross-sectional shape of hot-rolled sections, investigations were carried out on the residual stress pattern of similar shapes in increased yield strengths, as this has been identified as a key parameter affecting the resistance to flexural buckling. Although the forthcoming prEN1993–1-14 [58] recommends the use of the ECCS residual stress model scaled by 235 MPa regardless of the yield strength, a validation was carried out based on recent residual stress measurements performed on similar hot-rolled wide flange shapes of different grades [55,60,61, 62,63], as shown in Fig. 4.

Fig. 4 confirms that there is no residual stresses increase with the yield strength. All residual stress measurements provide residual stress levels at flange tips that are lower than those predicted by the residual stress model. For the sake of a prospective study, this is assumed to be the case for grades above the practical range. Consequently, the residual stress model is conservative, and the finite element model is deemed appropriate for the numerical simulation of hot-rolled sections in mild and high-strength steel grades.

ASSESSMENT OF CURRENT RECOMMENDATIONS FOR S235 AND S460 GRADES

The buckling curve recommendations from the current and the new upcoming versions of EN1993–1-1 [15,17] are reported in Table 4.

As can be seen in Table 4, the current buckling curves for the weak axis were a bit optimistic and recent researches have demonstrated that they were not appropriate [51,64,65]; one lower buckling curve was seen as more suitable and the modification has been introduced in the new upcoming version FprEN1993–1-1 [17]. Therefore, the situation of 1976 in which one higher buckling curve was recommended for the high-strength steel grade once again applies for each geometrical limit and buckling axis. Before going further in the present study, numerical simulations of the two grades already covered in standards, i.e. S235 and S460, have been performed for the sake of confirmation of the above-mentioned recent research. The results are represented in Fig. 5.

According to Fig. 5, a reasonable fit is obtained by comparing results from the GMNIA FineLg analyses and the selected buckling curves from Eurocode, especially for height-to-width ratios above 1.2 given the mean values $\bar{x}$ are close to 1.0 (as defined in the methodology). In contrast, for height-to-width ratios below 1.2, the simulated buckling resistances are about 5 % higher on average than the prescribed Eurocode curves. It means that, even for S235 and S460, there is a small margin of improvement.

The reduction factor accounting for flexural buckling highly depends on the residual stress distributions, the geometrical imperfections, and the yield strength whereas the cross-section geometries have a negligible impact for a same geometrical limit / table row defined in Table 8.3 of FprEN1993–1-1:2022 [17]. This observation justifies the methodology to consider only a limited number of profiles for the different geometrical limits / table rows studied. Eventually, the reduction factor is only slightly affected by geometric tolerances, given the importance of the effect of initial imperfections, thus the inferences remain valid.

Published in : Engineering Structures (2024), vol. 315, 118460
DOI: 10.1016/j.engstruct.2024.118460
Status : Postprint (Author's version)

Table 4
Eurocode selection of buckling curves for flexural buckling according to [15,17].

Limits	Buckling about axis	EN1993-1-1:2005		FprEN1993-1-1:2022	
		S235-S275-S355-S420	*S460*	*S235-S275-S355-S420*	*S460 up to S700*
$h/b > 1.2$ / $t_f \leq 40$ mm	y-y	a	a_0	a	a_0
	z-z	b	a_0	b	a
$h/b \leq 1.2$ / $t_f \leq 100$ mm	y-y	b	a	b	a
	z-z	c	a	c	b

Numerical simulations for relative slenderness of 0.2 present a reduction factor $\chi < 1.0$, meaning that, for this boundary limit between stocky and slender columns, flexural buckling appears earlier than the yielding of the cross-section. This observation is in line with other research works pointing out a lower reduction factor for this boundary slenderness [29,37]. Indeed, whatever the constitutive law, the consideration of the strain hardening has no impact for $\bar{\lambda} \geq 0.2$ [37]. These authors react to this feature by proposing a continuous imperfection factor which shifts the yielding plateau: Meng & Gardner [29] propose to reduce the yielding plateau from relative slenderness of 0.2 to 0.1 whereas Jonsson ̈ & Stan [37] even suggest a yielding plateau length which is a function of the yield strength, by applying the ε factor on the relative slenderness (see Table 2). In the framework of this research, following the mathematical model prescribed in prEN1993–1-14 [58], some simulations with a trilinear material law to account for strain hardening have been realized and the same peak loads were observed as shown in Fig. 6 for first slendernesses and selected profiles with height-to-width ratios above 1.2, confirming the observations expressed in the literature.

Fig. 6 testifies that the strain-hardening does not influence the results and the buckling load associated to relative slenderness of 0.2 is slightly lower than the member plastic resistance. Nonetheless, it is worth noting that the value of 0.2 has been prescribed based on experimental column tests which are likely to present lower imperfections than the ones conservatively used in numerical simulations. In addition, the yield strength is at least the nominal value and thus, it makes sense that this value results from statistical analyses of experimental tests instead of numerical simulations. For the sake of continuity with existing recommendations, it has been decided to keep the length of the plateau as it is suggested in Eurocode 3.

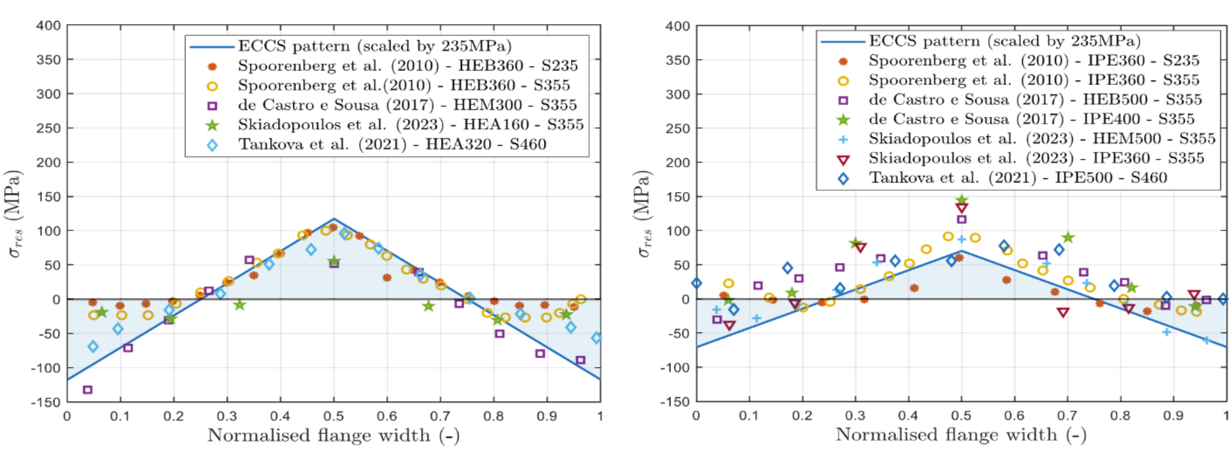

(a) h/b ≤ 1.2 (b) h/b > 1.2

Fig. 4. Validation of the residual stress model used in the numerical simulations.

Published in : Engineering Structures (2024), vol. 315, 118460
DOI: 10.1016/j.engstruct.2024.118460
Status : Postprint (Author's version)

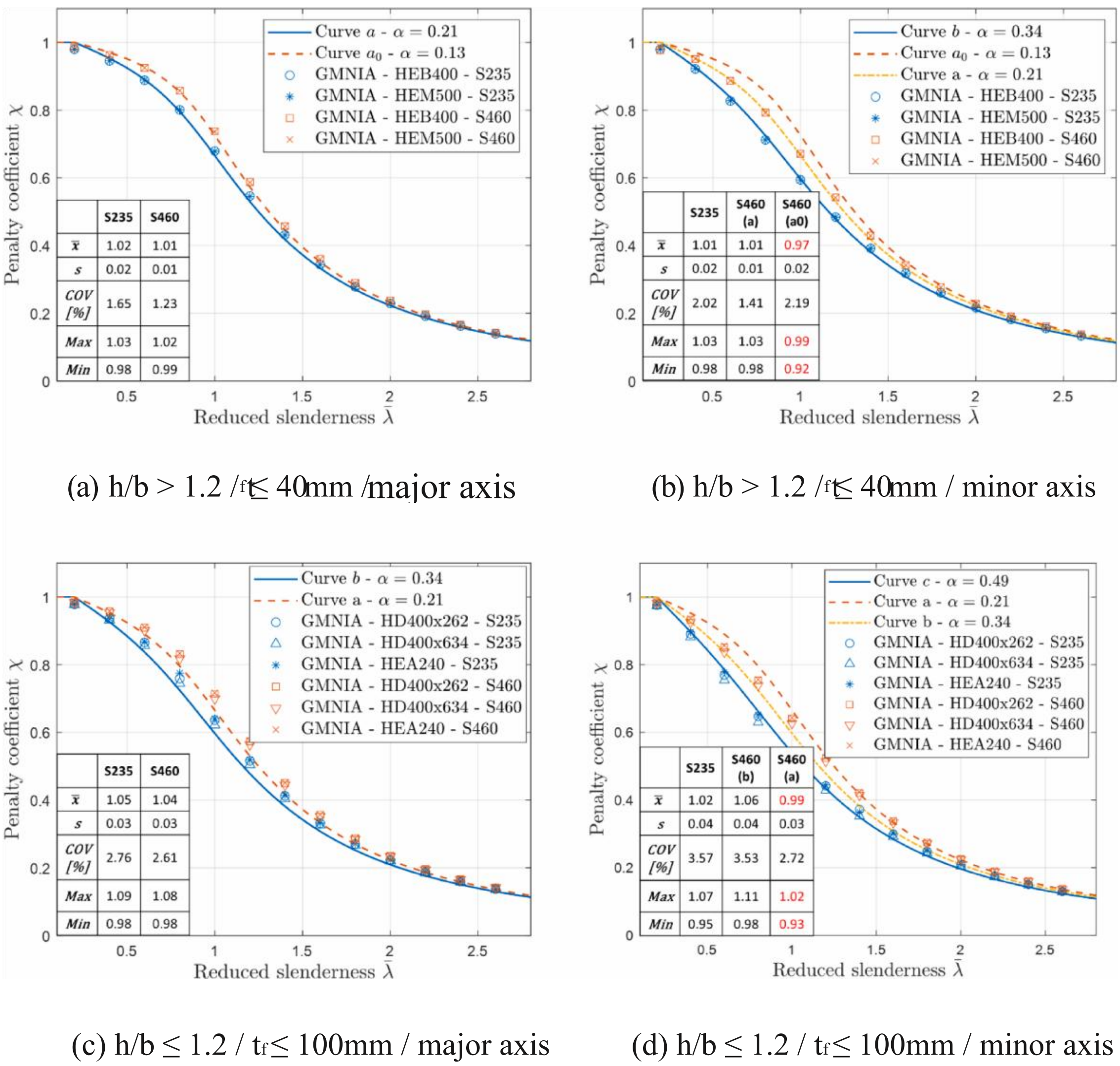

Fig. 5. Comparison between numerical simulations and Eurocode recommendations for S235 and S460.

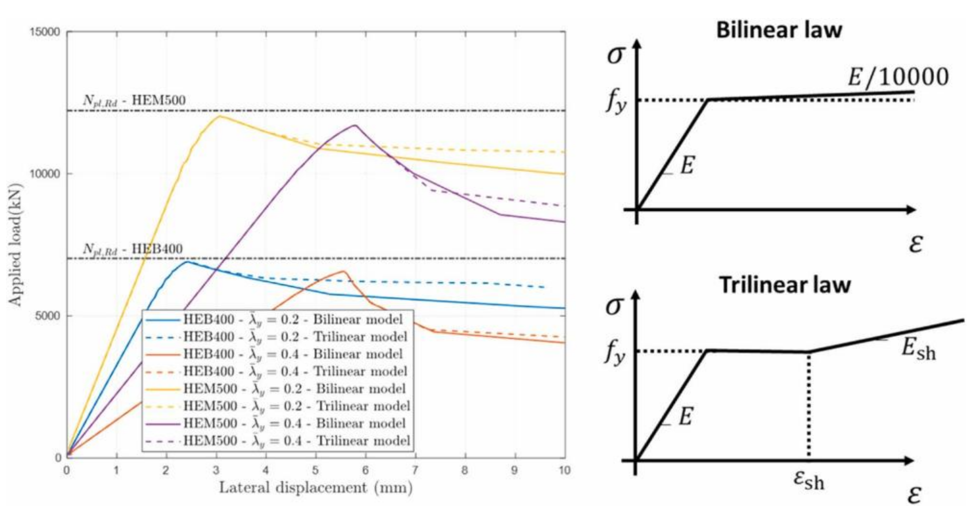

Fig. 6. Impact of strain-hardening on numerical simulations.

Published in : Engineering Structures (2024), vol. 315, 118460
DOI: 10.1016/j.engstruct.2024.118460
Status : Postprint (Author's version)

As explained in the literature, the modified Maquoi imperfection factor [26] fits with the jump of one buckling curve recommended at the time for 430 MPa (in previous ECCS recommendations [25]). The current version of EN1993–1-1 [15] sometimes offers a jump of two curves for S460, but it has been corrected in the last version FprEN1993–1-1 [17]. Indeed, a difference of one buckling curve between S235 and S460 is again prescribed in FprEN1993–1-1 [17], regardless of the h/b ratio and the buckling axis (Table 4). Consequently, given a jump of one buckling curve has been validated through numerical investigations and with the idea of conserving the length of the yielding plateau as it is, the approach of Maquoi [26] is adopted for establishing a new up-to-date imperfection factor.

CONSIDERATIONS FOR INTERMEDIATE GRADES (S355 AND S420)

As explained in the literature review and according to recent investigations [37,51], grades between S235 and S460 are probably the disadvantaged grades given the current Eurocode recommendations as the curve calibrated for S235 steel grade is imposed to the latter. These grades have been analyzed by representing the preconized buckling curve and the one just above to see whether a higher curve could be assigned to these grades (see Fig. 7). The statistical evaluation is made on this higher buckling curve i.e., curve a_0 in Fig. 7a, curve a in Fig. 7b and Fig. 7c and curve b in Fig. 7d.

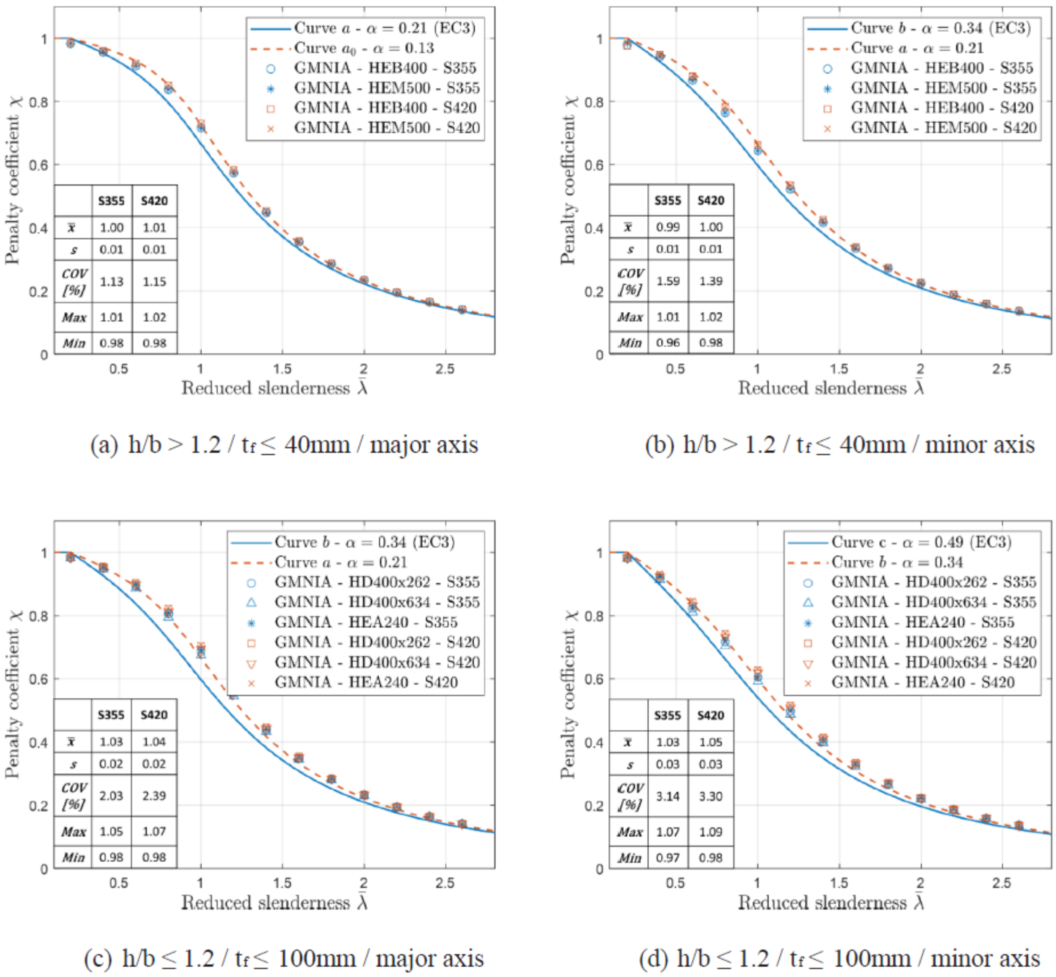

Fig. 7. Evaluation of the possibility of reducing one buckling curve for S355 and S420.

Published in : Engineering Structures (2024), vol. 315, 118460
DOI: 10.1016/j.engstruct.2024.118460
Status : Postprint (Author's version)

As demonstrated in Fig. 7, the results confirm the expectations that the buckling resistances of S355 and S420 are underestimated leading to over-designs for those grades. This observation is even more pronounced for height-to-width ratios below 1.2 as they encounter higher relative residual stress distributions. Whatever the height-to-width ratio, one higher buckling curve could have been prescribed for S355 and S420. However, the mean ratio χ is equal to or just below 1.0 for S355 in case of a height-to-width ratio beyond 1.2. The safety aspects should be discussed in the case of a higher curve selection. However, by defining a continuous imperfection factor, the increase could be less than one buckling curve, respecting in this case the statistical evaluation, as it will be demonstrated later on.

ESTABLISHMENT OF A CONTINUOUS EXPRESSION FOR THE IMPERFECTION FACTOR

Based on the research works presented in the previous subsections, it may be concluded that grades S235 and S460 are correctly characterized. The idea in this paper is therefore to propose a continuous imperfection factor, but strictly respecting the current recommendations for these two steel grades. It has been decided to consider the approach proposed by Maquoi [26], in which the exponent *n* is fixed equal to 0.7, to respect the current imperfection factors for S235 and S460 (Eq. 6). Indeed, by using this exponent, if $\alpha = 0.21$, $\alpha^* = 0.21$ for S235 and $\alpha^* = 0.13$ for S460. Similarly, if $\alpha = 0.34$, $\alpha^* = 0.34$ for S235 and $\alpha^* = 0.21$ for S460. These imperfection factors for S235 and S460 are in line with the current recommendations of Eurocode. However, if $\alpha = 0.49$, $\alpha^* = 0.49$ for S235 and $\alpha^* = 0.31$ for S460 which does not correspond to buckling curve "b". This difference was already stated for the Maquoi imperfection factor [26] and, it has been considered acceptable given the margin of improvement observed in Fig. 5d. So:

$$\alpha^* = \alpha * \left(\frac{235}{f_y}\right)^{0.7} \quad (6)$$

The study consists in evaluating for which α the buckling curve fits with the GMNIA results (corresponding to a mean value χ of 1.0 as defined in the methodology) considering a continuous vector of $\alpha \in [0.1 : 0.001 : 0.49]$. Fig. 8 illustrates the evolution of the calculated imperfection factor as a function of the yield strength and the proposed modified imperfection factor (Eq. 6) for the sake of comparison. In addition, results considering the minimum yield strengths prescribed in EN10025–2 and EN10025–4 [48,49] for profiles of Table 3 for which the thickness of the constitutive parts implies a yield stress reduction (see the strength reduction in Fig. 1) are also reported to evaluate the impact of this reduction on the results. For other cross-sections, the yield strength prescribed in Table 5.1 of FprEN1993–1-1 [17] is considered.

Published in : Engineering Structures (2024), vol. 315, 118460
DOI: 10.1016/j.engstruct.2024.118460
Status : Postprint (Author's version)

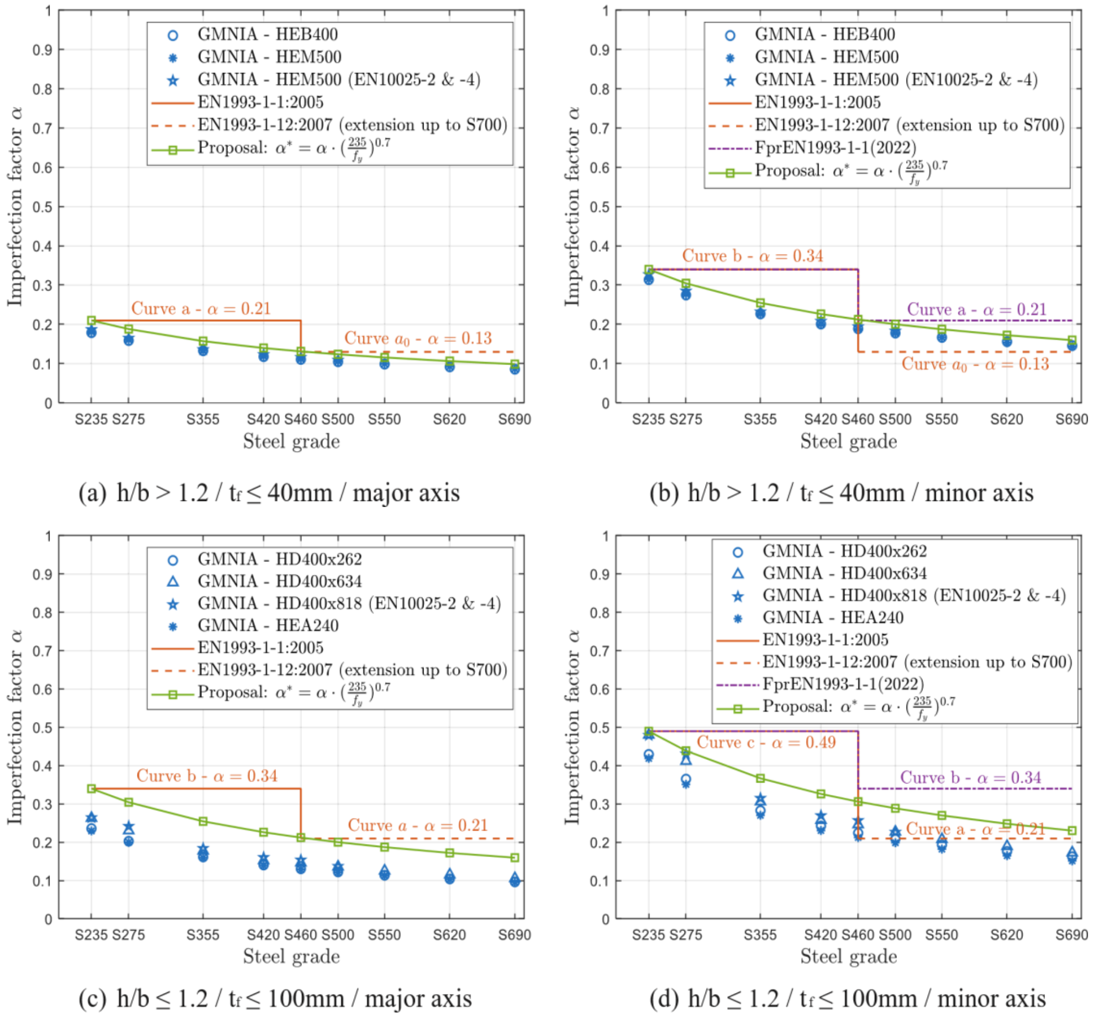

Fig. 8. Evolution of the imperfection factor α as function of the yield strength considering continuous buckling curves.

The consideration of sections with higher thicknesses according to EN10025–2 [48] and EN10025–4 [49] leads to higher imperfection coefficients which however remain below the corresponding modified imperfection factors of the proposal. Fig. 8 demonstrates the negligible impact of the yield strength up to flange thicknesses of 40 mm; this is in line with the recommendations of FprEN1993–1-1 [17] consisting of keeping the nominal yield strengths up to 40 mm. The proposal with an exponent of 0.7 gives a good correlation with numerical simulations.

This proposition offers a double advantage: (i) it provides a common buckling curve expression whatever the cross-section dimensions and the bucking axis, and (ii) it permits to conserve the historical Eurocode curves (a_0, a, b, c, and d) for S235.

Numerical simulations using shell finite elements

Considering high-strength steels for hot-rolled sections implies that some sections from producer catalogues fall into the class 4 cross-section category, meaning that they are susceptible to an earlier failure due to local plate buckling. So, some additional numerical simulations using shell finite elements have been realized to justify whether the modified imperfection factor is also valid for Class 4 cross-sections.

Published in : Engineering Structures (2024), vol. 315, 118460
DOI: 10.1016/j.engstruct.2024.118460
Status : Postprint (Author's version)

Geometrically and materially nonlinear analyses with imperfections (GMNIA) have been performed using the FineLg software [41]. The classical residual stress pattern as described in Fig. 9 is implemented, and two geometric imperfections are introduced based on a prior linear bifurcation analysis (LBA) performed on each member: a first geometric imperfection affine to the first flexural buckling mode shape and a second geometric imperfection affine to the first local buckling mode shape (see Fig. 9). The flexural buckling mode shape is amplified by L/1000 while the local buckling mode shape is amplified by c/200 as recommended in current EN1993–1-5 [66], in future upcoming recommendations for numerical modelling prEN1993–1-14 [58] and by other researchers [29]. Whilst some design recommendations preconize to reduce the amplitude of accompanying imperfections, no reduction has been applied in the present study for the sake of conservatism.

The investigations focus on two profiles, i.e., HEB600 and HEA300 in S460 and S690 subjected to flexural buckling about the weak axis; these profiles are Class 4 for yield strengths higher than 460 MPa due to the slenderness of their webs. The shell modelling implies an overlapping of the web over the flanges to have a mesh continuity and it has been chosen to neglect the fillets. A comparison of geometrical properties shows a difference of less than 0.1 % in terms of weak-axis moment of inertia; this difference is, therefore, negligible for weak-axis buckling. However, neglecting the fillets leads to a non-negligible reduction in the cross-sectional area, particularly for the lighter section (HEA300). Consequently, the reduced area used in simulations, noted A_{FEM}, has been considered for determining the specimen lengths (Eq. 4). A mesh sensitivity study has been realized and the mesh represented in Fig. 9 appears to be suitable to correctly model the instability phenomena (aspect ratios close to 1). Eventually, support conditions have been applied through kinematic coupling constraints at column ends, represented by dashed lines on the cross-section mesh in Fig. 9. The numerical modelling assumptions are summarized in Fig. 9.

The numerical campaign covers 52 columns which have been modelled for 2 grades (S460 and S690) and 13 slendernesses for each profile. The comparison with the modified imperfection factor curve is represented in Fig. 10 with a statistical evaluation.

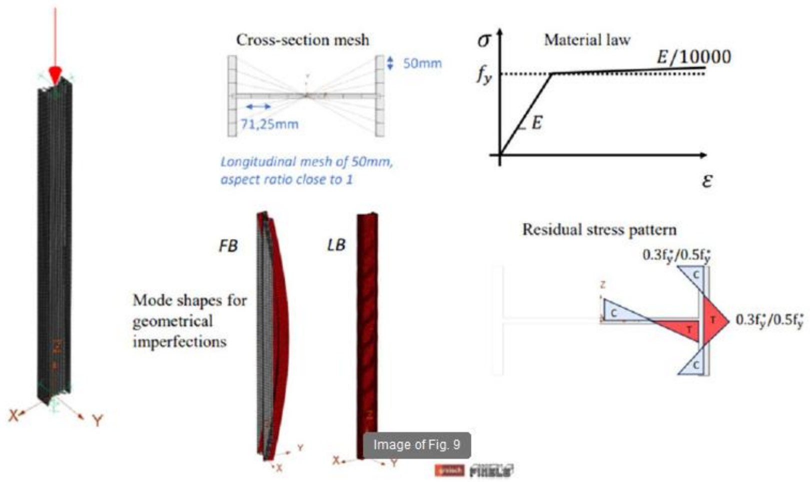

Fig. 9. Description of model assumptions for shell finite element modelling.

According to Fig. 10, it appears that similar results are observed between shell and beam finite element modelling, small differences are nonetheless observed in the intermediary slenderness range ($\bar{\lambda} \in [0.5\ 1.5]$). This can be justified by the superposition of the local plate imperfection in addition to the one associated with flexural buckling which may,

Published in : Engineering Structures (2024), vol. 315, 118460
DOI: 10.1016/j.engstruct.2024.118460
Status : Postprint (Author's version)

in some cases, increase or decrease the amplification factor of L/1000. However, the difference between both finite element simulations is seen as negligible. The statistical evaluation testifies of a good correlation between the shell model and the modified buckling curve proposal meaning that this proposition is also valid for class 4 cross-sections.

In addition, Fig. 10b also demonstrates that, even if the proposal does not perfectly respect a "jump" of one buckling curve in the case where $\alpha =$ 0.49 for S235, there is a good correlation between this imperfection factor proposal and the numerical results for S460, i.e., for $\alpha^* =$ 0.31.

Confrontation with other existing expressions from literature and benefit in terms of column buckling loads

Comparisons based on the mean value of the ratios of the buckling reduction factors from the proposal and other modified imperfection factors proposed in the literature, i.e., the average values $\overline{x}$ of $\frac{\chi_{FEM}}{\chi_{EC3}}, \frac{\chi_{FEM}}{\chi_{FprEN}}, \frac{\chi_{FEM}}{\chi_{Maquoi}}$ and $\frac{\chi_{FEM}}{\chi_{Jönsson}}$ are reported in Fig. 11.

Current and future upcoming versions of Eurocode recommendations provide valid design recommendations for S235 and S460 but completely neglect the beneficial impact of yield strength for intermediary grades and future emerging grades (yield strengths higher than 460 MPa).

Whilst Jonsson ¨ & Stan [37] focused on hot-rolled sections vulnerable to strong axis buckling only, the application of this modified factor for weak axis has also been evaluated. However, even for strong axis buckling, the mean value $\overline{x}$ is sometimes below the unity. The partial safety coefficient γ_{M1} = 1.0 should in this case be revised to be on the safe side. Additionally, the mean value $\overline{x}$ is always below unity for grades beyond S460 for weak axis buckling. According to Fig. 11, this criterion seems to be fully applicable up to 420 MPa but, beyond this grade, it is more questionable, especially for weak axis buckling.

Regarding the modified imperfection factor of Maquoi [26], the results are good, especially for grades below S460. In addition, this factor was calibrated in such a way that the curves adjust themselves on the classical imperfection factors from Table 1 for 235 MPa and 430 MPa; the proposal of this paper is just an adjustment of this factor for 460 MPa instead of the 430 MPa. Indeed, as can be seen in Fig. 11, the proposal of Maquoi [26] does not respect the current recommendations for S460 which were evaluated as suitable in this paper.

The adaptation of this factor with an exponent of 0.7 gives quite interesting results, with mean values $\overline{x}$ which do not exceed 5 % for height-to-width ratios below or equal to 1.2 while the mean values $\overline{x}$ are lower than 1.02 for height-to-width ratios beyond 1.2. This proposal could therefore enable each grade of the range covered by new up-coming standards to benefit from the beneficial effect of yield strength linked to the decreasing relative importance of the residual stresses, assuming the production process for these new steels will result in similar residual stress levels. In addition, this proposal respects the jump of one buckling curve between S235 and S460, except in the case where $\alpha =$ 0.49, $\alpha^* =$ 0.49 for S235 but $\alpha^* =$ 0.31 for S460. However, even with $\alpha^* =$ 0.31 for S460, the mean value $\overline{x}$ remains above 1.0 with a reasonable COV coefficient as can be seen in Fig. 11d.

Finally, the benefits in terms of member buckling loads resulting from the use of the proposed modified imperfection factor instead of new upcoming Eurocode recommendations are represented in Fig. 12.

Published in : Engineering Structures (2024), vol. 315, 118460
DOI: 10.1016/j.engstruct.2024.118460

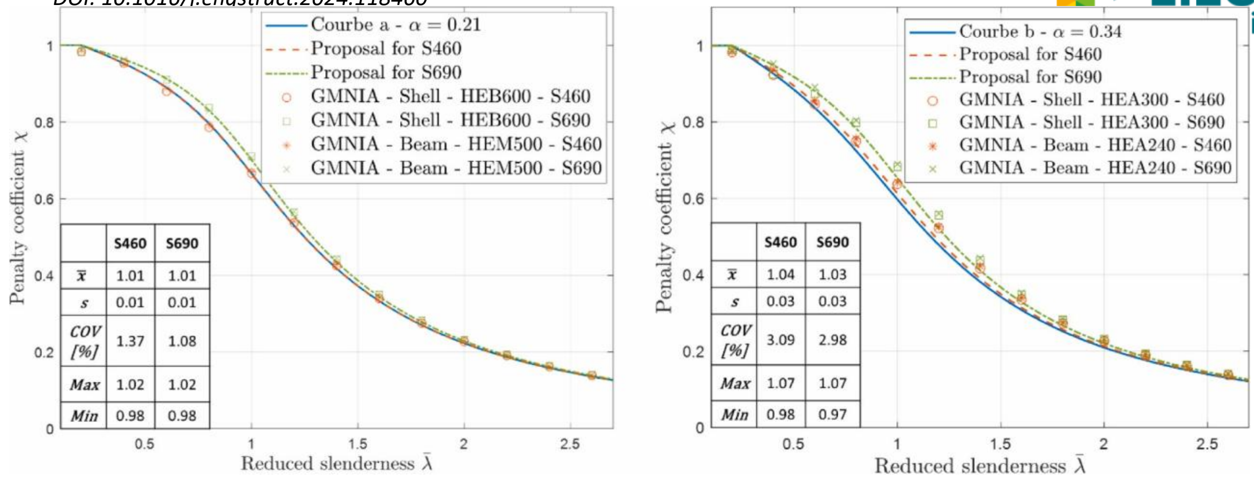

(a) $h/b > 1.2$ / $t_f \leq 40$mm / minor axis (HEB600) (b) $h/b \leq 1.2$ / $t_f \leq 100$mm / minor axis (HEA300)

Fig. 10. Comparison between shell numerical simulations and the modified imperfection factor for Class 4 cross-sections.

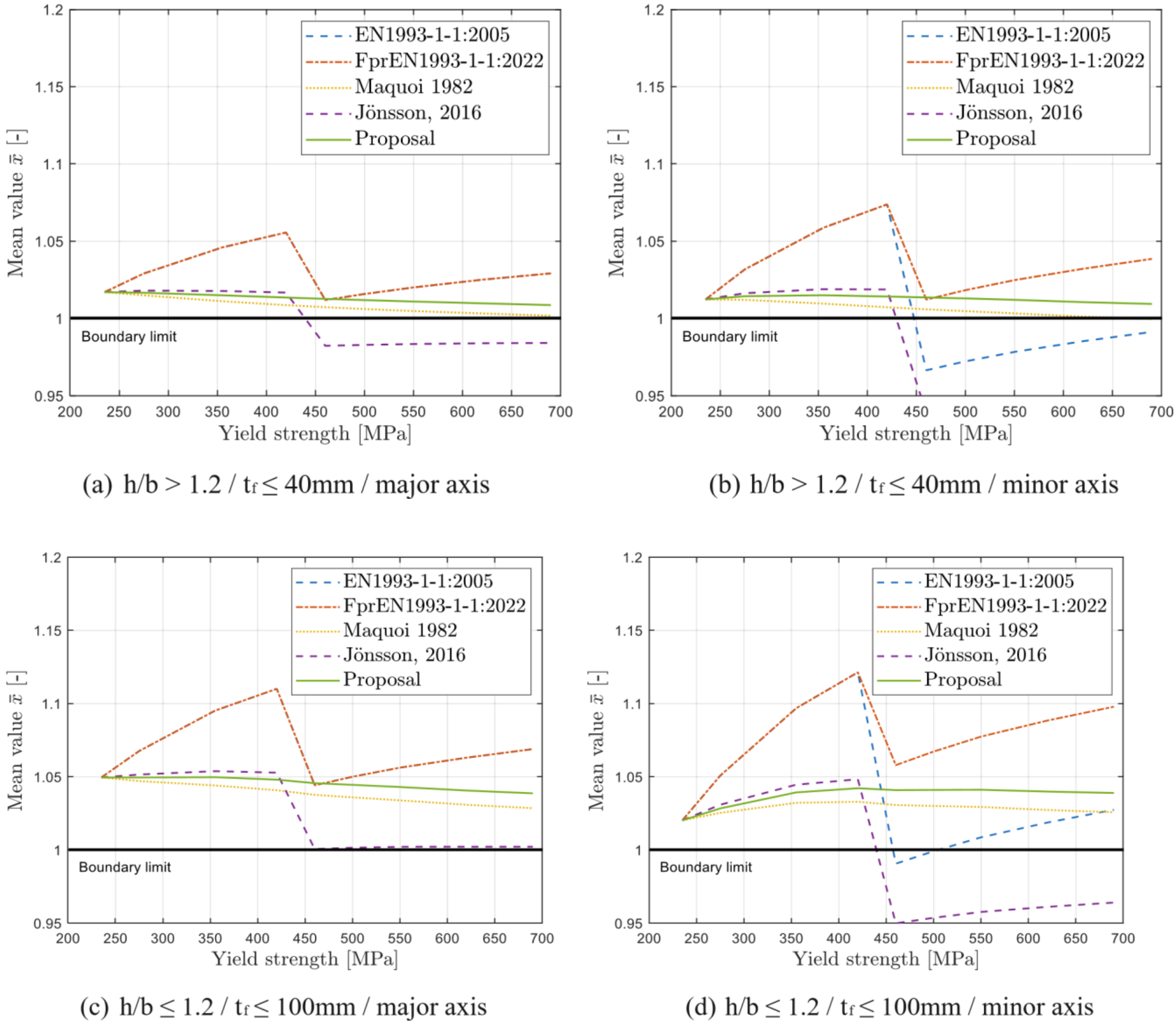

(a) $h/b > 1.2$ / $t_f \leq 40$mm / major axis (b) $h/b > 1.2$ / $t_f \leq 40$mm / minor axis

(c) $h/b \leq 1.2$ / $t_f \leq 100$mm / major axis (d) $h/b \leq 1.2$ / $t_f \leq 100$mm / minor axis

Fig. 11. Evolution of the mean values depending on the imperfection factor.

Published in : Engineering Structures (2024), vol. 315, 118460
DOI: 10.1016/j.engstruct.2024.118460
Status : Postprint (Author's version)

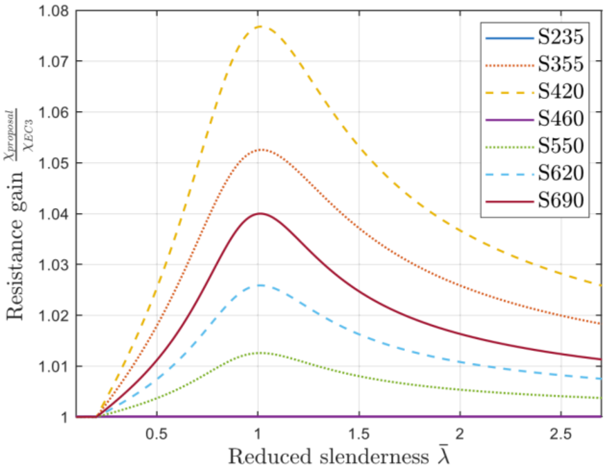

(a) Curve a

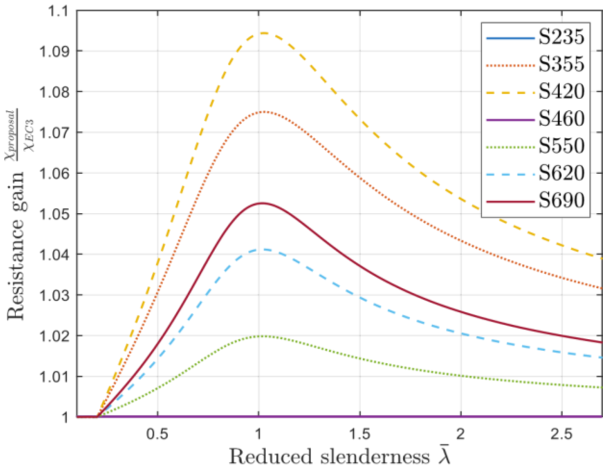

(b) Curve b

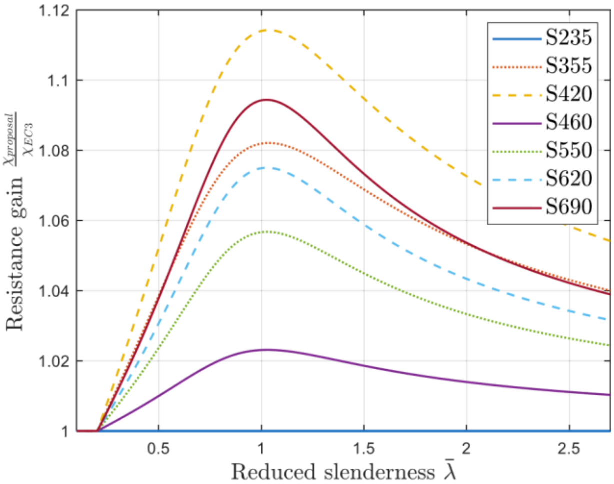

(c) Curve c

Fig. 12. Resulting gains from the use of the modified imperfection factor instead of new upcoming Eurocode recommendations [17].

Fig. 12 reports significant resistance increases especially for already existing grades S355 and S420 for which the flexural buckling resistances are currently underestimated in Eurocode. The peak increase corresponds to a non-dimensional slenderness of 1.0, for which the residual stresses distribution highly affects the results. The resistance gain is ranging from 1 to 12 % but, even a small increase in the buckling resistance may lead to a gain of one profile, and thus to a non-negligible reduction of the structure weight. Moreover, this modification contributes to the improvement of existing design rules, avoiding a non- physically justified stepwise evaluation of the buckling resistance when yield stress increases, and consequently, it contributes to the global objective of reducing the use of materials in future steel structures.

Published in : Engineering Structures (2024), vol. 315, 118460
DOI: 10.1016/j.engstruct.2024.118460
Status : Postprint (Author's version)

Conclusions

This paper proposes an adaptation of the design rules provided in Eurocode 3 for a member under pure compression prone to flexural buckling through the use of a modified and continuous expression of the so-called imperfection factor.

A review of the literature reveals that different authors have already suggested the use of a continuous expression of the imperfection factor. However, at present, the current and forthcoming version of Eurocode 3 still proposes a stepwise evolution of the imperfection factor by regrouping steel grades, which does not make physical sense.

This article presents the results of numerous numerical simulations aimed at providing the buckling resistance of hot-rolled columns for various existing or not yet existing grades as a prospective study. These simulations allowed to derive a continuous expression of the imperfection factor accounting for the decrease of the influence of the residual stresses on the flexural buckling resistance when the yield strength increases. The proposed modification is summarized in Fig. 13.

This factor is a slight modification of an existing modified imperfection factor proposed by Maquoi in 1982 [26], respecting the present normative recommendations made for S235 and S460 steel grades, which can be considered appropriate. This factor presents the second advantage to be applicable for all section dimensions covered in this paper. The classical buckling curves recommended in Table 1 are conserved for grade S235, while the yield strength is accounted for by a modified imperfection factor. All grades beyond S235 would thus be freed from any undue penalization caused by a non-continuity of design recommendations in terms of imperfection factors.

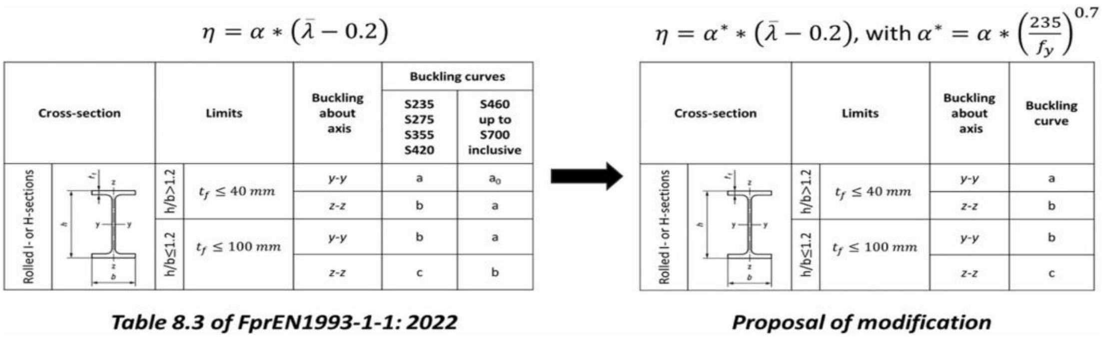

Fig. 13. Summary of the modification proposal.

Although this article initially focused on high-strength steels, it was demonstrated that several existing grades were also disadvantaged by current rules. It is particularly the case for steel grade S355 for which the flexural buckling resistance is currently underestimated. In the context of growing issues in terms of resource scarcity, it becomes crucial to adapt the design rules to optimize the material usage in the building sector.

This proposal is the result of a theoretical study; Monte-Carlo simulations may be carried out to take into account the variability of geometrical and material properties. Experimental column tests would also make it possible to carry out a statistical study and set the associated partial safety coefficient γ_{M1} according to annex D of EN 1990, especially tests on grades equal to or higher than 500 MPa which could appear in the upcoming years to validate the proposed trend. Finally, existing modified imperfection factors for hollow sections or welded I-beams should be analyzed to investigate the possibility of having the same expression for the imperfection factor whatever the section typology.

Published in : Engineering Structures (2024), vol. 315, 118460
DOI: 10.1016/j.engstruct.2024.118460
Status : Postprint (Author's version)

CRediT authorship contribution statement

Loris Saufnay: Writing – original draft, Visualization, Validation, Resources, Methodology, Investigation, Formal analysis. **Jean-Pierre Jaspart:** Supervision, Methodology. **Jean-François Demonceau:** Writing – review & editing, Supervision, Project administration, Methodology.

Declaration of Competing Interest

The authors declare that they have no known competing financial interests or personal relationships that could have appeared to influence the work reported in this paper.

Data Availability

Data will be made available on request.

References

[1] Worldsteel Association, Steel in the circular economy: A life cycle perspective, Brussels, 2015.

[2] Saufnay L, Demonceau J-F. Establishment of reliable relative price predictions for high-strength steel members. Steel Constr 2023. https://doi.org/10.1002/stco.202300013.

[3] Saufnay L, Demonceau J-F. Economic and environmental assessment of high- strength steel grades. ce/Pap 2023;vol. 6(3–4):527–32.

[4] D. Dubina et al., High Strength Steel in Seismic Resistant Building Frames (HSS- SERF), Luxembourg, 2015 [Online]. Available: 〈https://op.europa.eu/en/publication-detail/-/publication/89c1799c-017f-417b-b913–5369cbfeb45e/language-en〉 .

[5] N. Baddoo et al., High strength long span structures (HILONG): Final report, 2017 [Online]. Available: 〈https://op.europa.eu/en/publication-detail/-/publication/de c2dad6–47a4–11e7-aea8–01aa75ed71a1〉 .

[6] M. Veljkovic et al., High-strength tower in steel for wind turbines (HISTWIN2): Final report, 2015 [Online]. Available: 〈https://op.europa.eu/en/publication-detail/-/publication/ b5387d03-c2ad-4e9a-95a2–70172513d84b/ language-e n/format-PDF/source-209815554).

[7] M. Feldmann et al., Rules on high strength steels (RUOSTE): Final report, 2016 [Online]. Available: 〈https://op.europa.eu/en/publication-detail/-/publication/515285b0-c820–11e6-a6db-01aa75ed71a1〉 .

[8] M. Veljkovic et al., High-strength tower in steel for wind turbines (HISTWIN): Final report, 2012 [Online]. Available: 〈https://op.europa.eu/en/publication-detail/-/publication/1081fa93%E2%80%930319-4710-a16c-08692a5f5265/language -en/format-PDF/source-209815516〉 .

[9] A.-M. Habraken et al., Optimal use of high strength steel grades within bridges (OPTIBRI): Final report., 2019 [Online]. Available: 〈https://op.europa.eu/en/publication-detail/-/publication/d8bd0ac1–4479-11e9-a8ed-01aa75ed71a1/langua ge-en〉 .

[10] Vayas et al., Innovative solutions for design and strengthening of telecommunications and transmission lattice towers using large angles from high strength steel and hybrid techniques of angles with FRP strips (ANGELHY): Final report, 2021.

[11] N. Baddoo et al., Stronger steels in the built environment (STROBE): Final report, 2021.

[12] Collin P, Johansson B. Eur High Strength Steel Appl Constr 2005.

[13] Stroetmann R. "High strength steel for improvement of sustainability. Proc 6th Eur Conf Steel Compos Struct, Proc 2011:31.

[14] Saufnay L, Jaspart J, Demonceau J. Economic benefit of high strength steel sections for steel structures. ce/Pap 2021;vol. 4(2–4):1543–50. https://doi.org/10.1002/cepa.1454.

[15] CEN, "EN1993–1-1:2005: Eurocode 3: Design of steel structures - Part 1–1: General rules and rules for buildings," Brussels, 2005.

[16] CEN, "EN1993–1-12:2007: Eurocode 3 - Design of steel structures - Part 1–12: Additional rules for the extension of EN 1993 up to steel grades S 700.," Brussels, 2007.

[17] CEN, "FprEN1993–1-1:2022: Eurocode 3: Design of steel structures - Part 1–1: General rules and rules for buildings," Brussels, 2022.

[18] Sfintesco D. Fondement experimental des courbes européennes de flambement. Constr métallique 1970;vol. 3:5–12.

[19] Beer H, Schulz G. Bases théoriques des courbes européennes de flambement. Constr Métallique 1970;vol. 3(485):37–57.

[20] Strating J, Vos H. Computer Simulation of the ECCS Buckling Curve using a Monte- Carlo Method. Constr Metallique 1973;vol. 2:2´ 3–39.

[21] Maquoi R, Rondal J. Mise En équation Des Nouv Courbes Eur De flambement 1978.

[22] Jasinski F. Recherches sur la flexion des pièces comprimées. Vve Ch. Dunod & P. Vicq; 1894.

[23] Fukumoto Y, Itoh Y. Evaluation of multiple column curves using the experimental data-base approach. J Constr Steel Res 1983;vol. 3(3):2–19.

[24] Lee C-H, Han K-H, Uang C-M, Kim D-K, Park C-H, Kim J-H. Flexural strength and rotation capacity of I-shaped beams fabricated from 800-MPa steel. J Struct Eng 2013;vol. 139(6):1043–58.

[25] ECCS, Manual on stability of steel structures. S. l: [s. n.], 1976.

[26] Maquoi R. Some improvements to the buckling design of centrally loaded columns. Struct Stab Res Counc, Proc Annu Meet 1982.

[27] R. Maquoi and J.-P. Jaspart, Quelques réflexions a propos des courbes de ` flambement et de l'amplitude relative d'imperfection géométrique équivalente," Liège, Dec. 2016.
[28] G. Sedlacek, "Buckling behaviour of hot-formed SHS in high strength steel grade E- 460. Comité international pour le développement et l'étude de la construction tubulaire," 1999.
[29] Meng X, Gardner L. Behavior and design of normal-and high-strength steel SHS and RHS columns. J Struct Eng 2020;vol. 146(11):4020227.
[30] Wang J, Gardner L. Flexural buckling of hot-finished high-strength steel SHS and RHS columns. J Struct Eng 2017;vol. 143(6):4017028.
[31] Rasmussen KJR, Hancock GJ. Tests of high strength steel columns. J Constr Steel Res 1995;vol. 34(1):27–52.
[32] Ma T-Y, Liu X, Hu Y-F, Chung K-F, Li G-Q. Structural behaviour of slender columns of high strength S690 steel welded H-sections under compression. Eng Struct 2018; vol. 157:75–85.
[33] Li T-J, Li G-Q, Chan S-L, Wang Y-B. Behavior of Q690 high-strength steel columns: Part 1: experimental investigation. J Constr Steel Res 2016;vol. 123:18–30.
[34] Sabau G, Lagerqvist O, Baddoo N. Statistical analysis of flexural-buckling- resistance models for high-strength steel columns. J Struct Eng 2020;vol. 146(2): 4019210.
[35] Shi G, Ban H, Bijlaard FSK. Tests and numerical study of ultra-high strength steel columns with end restraints. J Constr Steel Res 2012;vol. 70:236–47.
[36] Ban H, Shi G, Shi Y, Wang Y. Overall buckling behavior of 460 MPa high strength steel columns: experimental investigation and design method. J Constr Steel Res 2012;vol. 74:140–50.
[37] Jonsson J, Stan T-C. European column buckling curves and finite element modelling including high strength steels. J Constr Steel Res 2017;vol. 128:136–51.
[38] Somodi B, Kovesdi B. Flexural buckling resistance of cold-formed HSS hollow section members. J Constr Steel Res 2017;vol. 128:179–92.
[39] Somodi B, Kovesdi B. Flexural buckling resistance of welded HSS box section members. Thin-Walled Struct 2017;vol. 119:266–81.
[40] Johansson B. Buckling Resistance of Structures of High Strength Steel, in Use and application of high-performance steels for steel structures. IABSE, Int Assoc Bridge Struct Eng (IABSE) 2005:120–8.
[41] Greisch office and University of Liege, "FineLg: non-linear finite element analysis program: user's manual." Liège, Sep. 2018.
[42] V. de Goyet, "L'analyse statique non linéaire par la méthode des éléments finis des structures spatiales formées de poutres a section non symétrique," Université de Liege, 1989. `
[43] Boissonnade N, Degée H, Naumes J, Oppe M. Experimental and numerical investigations for I-girders in bending and shear stiffened by trapezoidal stiffeners. Adv Steel Constr 2008;vol. 4(1):1–12.
[44] Boissonnade N, Somja H. "Influence of imperfections in FEM modeling of lateral torsional buckling. Proc Annu Stab Conf 2012:18–21.
[45] Bezas M-Z, Demonceau J-F, Vayas I, Jaspart J-P. Experimental and numerical investigations on large angle high strength steel columns. Thin-Walled Struct 2021; vol. 159:107287. https://doi.org/10.1016/j.tws.2020.107287.
[46] Bezas M-Z, Demonceau J-F, Vayas I, Jaspart J-P. Design rules for equal-leg angle members subjected to compression and bending. J Constr Steel Res 2022;vol. 189: 107092.
[47] ArcelorMittal, HISTAR®: Innovative high strength steels for economical steel structures, 2020[Online]. Available: 〈https://sections.arcelormittal.com/repository2/Sections/5_3_1_HISTAR_web.pdf〉.
[48] NBN, "EN10025–2:2019: Hot-rolled products of structural steels, part 2: Technical delivery conditions for non-alloy structural steels," Brussels, 2019.
[49] NBN, "EN10025–4:2019: Hot-rolled products of structural steels, part 4: Technical delivery conditions for thermomechanical rolled weldable fine grain structural steels," Brussels, 2019.
[50] Snijder HH, Cajot L-G, Popa N, Spoorenberg RC. Buckling curves for heavy wide flange steel columns. Rom J Tech Sci: Appl Mech 2014;vol. 59(1/2):178–204.
[51] da Silva LS, Tankova T, Marques L, Rebelo C. Safety assessment of Eurocode 3 stability design rules for the flexural buckling of columns. Adv Steel Construction–Int J 2016;vol. 12(3):328–58.
[52] Mathworks, MATLAB version R2019b. Natick, Massachusetts, 2019.
[53] Young BW. Residual Stresses in Hot-rolled Sections. University of Cambridge; 1971.
[54] Tankova T, da Silva LS, Rodrigues F. Buckling curve selection for HSS welded I- section members. Thin-Walled Struct 2022;vol. 177:109430.
[55] Skiadopoulos A, Sousa A de C e, Lignos DG. Experiments and proposed model for residual stresses in hot-rolled wide flange shapes. J Constr Steel Res 2023;vol. 210: 108069.
[56] G.A. Alpsten, Variations in mechanical and cross-selectional properties of steel. na, 1973.
[57] Lindner J, Kuhlmann U, Just A. Verification of flexural buckling according to Eurocode 3 part 1-1 using bow imperfections. Steel Constr 2016;vol. 9(4):349–62.
[58] CEN, "prEN1993–1-14: Eurocode 3: Design of steel structures — Part 1–14: Design assisted by finite element analysis, Brussels, Jan. 2021.
[59] Tebedge N, Chen WF, Tall L. Experimental studies on column strength of european heavy shapes. Fritz Eng Lab Rep No Nov. 1972;351(7).
[60] Spoorenberg RC, Snijder HH, Hoenderkamp JCD. Experimental investigation of residual stresses in roller bent wide flange steel sections. J Constr Steel Res 2010; vol. 66(6):737–47.
[61] A.A. Sousa and D. Lignos, Residual stress measurements of European hot-rolled I- shaped steel profiles, 2017.
[62] A. Skiadopoulos, A. de Castro e Sousa, D. Lignos, "Database of Residual Stress Measurements on Hot-rolled Wide Flange Steel Cross Sections," 2023.
[63] Tankova T, Rodrigues F, Leitao C, Martins C, da Silva LS. Lateral-torsional buckling of high strength steel beams: experimental resistance. Thin-Walled Struct 2021;vol. 164:107913.
[64] J. Lindner and L. da Silva, "Classification of rolled I-Profiles fabricated in steel grade S460 within Table 6.2 of EN 1993–1-1," 2015.
[65] Snijder HH. Recent developments regarding the next version of Eurocode 3 part 1-1 on steel structures. ce/Pap 2017;vol. 1(4):515–38.
[66] CEN, "EN1993–1-5: Eurocode 3: Design of steel structures – Part 1–5: Plated structural elements," Brussels, 2005.